Large-scale brain networks get entrained during processing of periodic auditory stimuli

by

Neeraj kumar

A Dissertation Submitted to the Faculty of

The National Brain Research Centre in Partial

Fulfillment of the Requirements for the Masters in Neuroscience

National Brain Reserach Centre

Manesar, Gurugram, Haryana

May 2017

CERTIFICATE

This is to certify that the Dissertation entitled *"Large-scale brain networks get entrained during processing of periodic auditory stimuli"* was carried out by Mr. **Neeraj kumar** at National Brain Research Centre, (Deemed University), Manesar, Haryana, as the partial fulfilment for the M.Sc. degree.

The work presented herein is original and has not been submitted previously for the award of any degree or diploma at National Brain Research Centre (Deemed University) or any other University.

Supervisor Director

Place: Manesar

Date: 31 May, 2017

DECLARATION BY THE CANDIDATE

I **Neeraj kumar** hereby declare that the work presented in this dissertation is carried out by me, under the guidance of **Dr. Arpan Banerjee** National Brain Research Centre, (Deemed University), Manesar, Haryana.

I also declare that no part of this dissertation has been previously submitted for the award of any degree or diploma at National Brain Research Centre (Deemed University) or any other University.

Neeraj kumar

M.Sc. final

Place: Manesar

Date: 31 May, 2017

ACKNOWLEDGEMENT

Foremost, I would like to express my sincere gratitude to my advisor Dr.Arpan Banerjee for the continuous support of my MSc. Dissertation work. Without his guidance and dedicated involvement at every step throughout my dissertation, this undertaking would have never been accomplished. The door to Arpans office was always open whenever I ran into a trouble spot or had a question regarding my research. Thanks for being a supportive guide Arpan !

My special thanks goes to Vinodh G Kumar who taught me various tools and methods with great deal of patience at various stages of my training.

My work at Cognitive Brain lab would have been difficult without valuable help from my labmates. Thank you Amit Ranjan, Anirudh, Dipanjan, Dr.Amit Naskar, Nilambari, Priyanka, Shrey, Siddharth, Shyamchand and former lab members especially Tamesh Haldar for the stimulating discussions we had in lab.

A special word of gratitude goes to Amit Jaiswal who helped me over facebook chats in learning and designing my work.

My heartfelt thanks goes to Meenakshi and Surajit for continuous encouragement in all odd times and for the sleepless nights we were working together before deadlines. Lastly, I would like to thank my batchmates for all the fun we had in the last two years.

My deep sense of gratitude goes to almighty for his countless love and my parents who supported me throughout my life.

Neeraj Kumar

Abstract

Author:	Neeraj kumar
Title:	Large-scale brain networks get entrained during processing of periodic auditory stimuli
Institution:	National Brain Reserach Centre
Dissertation Advisor:	Dr. Arpan Banerjee
Degree:	Masters in Neuroscience
Year:	2017

In the real world we are bombarded with a range of acoustic stimuli having a number of frequencies. Several electroencephalogram (EEG) studies have shown that stimulation by periodic auditory stimuli evokes a steady state response at the corresponding frequency, with 40Hz eliciting maximum response. Despite having enormous potential for clinical applications from measuring hearing threshold to characterizing the alteration of diseased state in Alzheimer's, the underlying network mechanisms are poorly understood. Present study exploits this paradigm to characterize the network mechanisms underlying binaural and monaural auditory stimulation.

Subjects were presented with binaural and monaural stimuli. Pure tones at 1kHz frequency were presented at 40 cycles a second during the periodic stimulation period. I observed the enhancement of spectral power at individual participant and group level at 40 Hz in distributed scalp sensor locations. Maximum 40 Hz spectral power found in mastoid sensors and frontal central areas. Subsequently, I computed global coherence, an average of all of the pairwise coherences, to identify the presence of a large-scale brain network. Task-specific enhancement of global coherence specifically at 40 Hz indicates the entrainment of a large-scale neuronal network in monaural and binaural conditions. Hemispheric analysis revealed the ipsilateral dominance in the processing of monaural stimuli. Subsequently, measurement of pairwise imaginary coherence to detect sub-networks were carried out. Statistical testing of interaction among channel pairs was done using non-parametric tests. Bilateral long range interactions involving centro-frontal and temporal sensors and parietooccipital sensors were significant. These interactions were ipsilateral dominant in monaural conditions. To identify the causal influence in all significantly interacting channel

pair I employed Granger causality (GC) analysis. In both monaural and binaural conditions, GC revealed the influence of right temporal region to the frontal areas. Furthermore, in binaural and monaural left condition GC indicates the unidirectional influence of frontal regions to left mastoid region.

In conclusion, I establish the presence of large-scale effective networks encompassing bilateral auditory and frontal areas that get entrained during the processing of 40 Hz auditory stimuli.

Contents

List of Figures

Chapter 1

Introduction

"There are billions of neurons in our brains, but what are neurons? Just cells. The brain has no knowledge untill connections are made between neurons. All that we know, all that we are, comes from the way our neurons are connected." - Tim Berners-Lee

Perception of the external world requires the processing of information incoming from the sense organs. The brain accomplishes this information processing primarily through detection, interpretation and action selection. However, majority of the incoming information in our daily lives encompasses a spectrum of features (such as alignment, periodicity, spatial frequency etc). Therefore, the brain performs the complex task of analyzing and uniting these features which enables us to gain a unified percept. Research directed towards understanding the mechanism of information processing primarily believe in localizationism or modular models [2, 3, 4]. Wherein they hypothesize in mapping specific brain areas to specific functions [5]. Nevertheless, higher order cognitive functions like speech perception, memory encoding, consciousness etc. require the involvement of multiple brain areas. Therefore, their mechanisms need to be explained under the framework of functional integration rather than segregation.

The functional integration concept hypothesize that coordinated activity of distributed neuronal assemblies underlie cognition. Such co-activated neuronal assemblies in response to any cognitive task form a network which are called the *neuro-cognitive networks* [6]. The spatio-temporal dynamics of these networks can be characterized from the pattern

of their electromagnetic and metabolic activity. In the current report, we explore the various measures by which we can compute the dynamics of the neuro-cognitive networks that entails any cognitive function.

1.1 Brain networks

Whenever brain is subjected to perform a certain task, areas involved in comprehending that activity are co-activated [7]. All the neuronal elements that are linked together to achieve a common goal are referred to as a **brain network**. A neuronal element can be represented as a neuron, a neuronal ensemble or a brain region. Coalitions of a set of neuronal elements during an exogenous or endogenous task, mark the emergence of a network. Dynamics of thus emerged network vary depending upon the information processing in the brain. Acquired information can be processed either temporally or spatially or by the interplay of both[8]. Two modes of neuronal connectivity are 1. Anatomical networks and 2. Functional networks.

1.1.1 Anatomical networks

By definition, anatomical networks are the ones that are based on the physical or structural links between different regions of the brain [9]. These links are created by connecting various neuronal hubs by synapse or axonal pathways. Axonal pathways have directionality associated with them due to polar nature of neurons. Synaptic plasticity is an important measurable parameter in anatomical connectivity which at a microscopic level is defined as change in synaptic strength over time [10]. In vitro tracing methods and in vivo diffusion tensor imaging (DTI) are one of the few popular techniques used for studying anatomical networks. Depending upon the plasticity of the brain and stimulus provided, changes in anatomical networks may take from minutes to years [11]. Structural plasticity occurs during making new experiences and learning processes [12, 13, 14]. .

1.1.2 Functional network

Functional connectivity is defined as the temporal dependency of neuronal activation patterns of anatomically separated brain regions [15, 16]. A functional network consists of

unique sets of transient interactions between neuronal elements (from individual neuronal to interactions in specialized brain areas). Temporal dynamics of a functional network change in the range of milliseconds [17, 18]. Furthermore, dynamics of functional networks are subject to vary with age [19]. This is a consequence of a change in the anatomical architecture across an individual's lifespan as described in the previous section. The Neuronal connection that consists long ranges interactions between functionally diverse brain areas are called large scale network. A well coordinated cognitive function is a consequence of large-scale functional networks. A functional network is thus detected by its role in the induction of a cognitive state.

1.2 Importance of brain networks

Once stimulated by some extrinsic or intrinsic stimuli corresponding brain network will activate. There are substantial evidence that suggests that large-scale brain networks are involved in each stage of neural information processing [20, 21, 22, 23, 24, 18, 25, 26]. Principle feature of a network is to provide a coordinated framework for the *functional integration* of information processing in distributed neuronal ensembles during higher order cognitive functions [27, 15]. Functional integration is crucial for multiple brains areas to simultaneously participate in information processing by modulating their interactions accordingly. Subsequently, they perform principal actions that include controlling other cortical or subcortical structures [28, 29], modulating the behavior of respective effector organs. Aforementioned actions can be performed by the whole network or can be divided into component regions. These networks also coordinate with networks of other modality to have an integrate. "Network hub", neuronal elements that have a high degree of connectivity (high participation coefficient) to the network of other modality, mediate the process of integration of information from distributed brain areas. Networks synchronization has been implicated to play a crucial role in perception, memory, and even consciousness [30, 31, 32, 33, 34]. In the absence of any task, brain attain resting state. The state of resting is also maintained by an explicit network termed as resting state network [35]. Out of many networks, default mode network(DMN) is most studied resting brain network. DMN which plays an important role in monitoring the internal mental landscape

[26]. Another popular network called salience network (SN), have a crucial role in maintaining attentional mechanisms to the most biologically and cognitively relevant events [36]. Dynamic interactions between brain areas provide a framework in a shift of attention [37]. For successful segregation and integration of information between specialized brain regions, an effective mechanism should be there. A network provides an architecture to accomplishing this. "Connector hub", neuronal structures that have very high degree of participation coefficient in a network have a role in intermodular communication. Thus provide a basis to understand the segregation and integration of information in the brain. A careful examination of the organization of functional networks results in similarities to small-world attributes [21]. This proves information transfer to other regions is not only fast but metabolically and economically efficient. Hence, a network provide an structural and functional architecture on which information flow or integrative processes occurs.

1.3 Tools for the extraction of brain networks

To understanding task specific dynamics of brain require the characterization of network mechanisms at varying spatiotemporal scales from neuroimaging data recorded at high temporal resolution. Recent neuroimaging techniques has catalyzed the evolution of functional connectivity measures that have potential to evaluate the spatiotemporal dynamics of neurocognitive networks. There are various established measures to asses functional connectivity from the empirical data. Major steps to estimate brain network from empirical data are summarized in figure 1.1. In the current, section we provide an overview of some measures used to estimate a network from empirical data.

1.3.1 Mapping of functional motifs

A functional network emerges from the *dynamic* interactions between specialized anatomical regions of the brain [38]. Hence to extract a particular network, underlying functional sources should be identified. A source corresponds to a brain region of enhanced activity in response to an endogenous or exogenous task. They act as functional units during information processing in the brain [39]. Hence, these sources must have an individual function during a cognitive task in addition to coactivation with other sources. Evaluating

the sources underlie any cognitive task using empirical data are highly dependent based on different assumptions about the underlying measure and the modality of the neuroimaging technique that was used.

The increased activity of sources can be identified using noninvasive neuroimaging techniques including, enhanced glucose metabolism in positron emission tomography (PET), enhanced blood flow in functional magnetic resonance imaging (fMRI), recordings or synchronized oscillatory activity in electroencephalography (EEG) and magnetoencephalography (MEG) recordings. Studies on task-evoked network have compared enhanced activity with the baseline state. i.e. when the brain is at rest. Enhancement is evaluated for significance by statistical testing. Statistical parametric mapping (SPM), is a widely used software that provides a range of methods for assessing the difference in brain activities recorded during fMRI. In other cases, depending upon the nature of study, enhanced activity is compared with the baseline, other cognitive task or interindividual differences. In the present work, EEG recording was used to identify the sources of activation in the brain.

1.3.2 Estimation of connectivity from neuroimaging time series

Time series refers to the neuroimaging signal in the time domain. Non-invasive neuroimaging methods provide simultaneous recording from multiple brain areas. Additionally, presence of high temporal resolution makes EEG/MEG time series data very rich in oscillatory content. Hence, providing a good base for establishing statistical dependencies between observed time series (functional connectivity). Information processing during higher order cognitive processes requires the functional integration of distributed brain areas. There are multiple ways to explore the dynamics of integration in a functional network during a cognitive task. The first step in the use of time series to evaluate the functional connectivity started by calculating the cross-correlation. In cross-correlation, time series from one channel of EEG/MEG is compared with simultaneously recorded time series of another channel. Measuring correlation at each lag, i.e., (cross-correlation) assists in determining the functional connectivity [40]. It is until 1965 when Cooley and Tukey introduced the concept of Fourier transform. A mathematical algorithm that decomposes a time series into its constituent frequency component, made up of sine waveforms [41]. Use of Fourier transform in calculating spectral coherence, correlation in the frequency domain was exploited

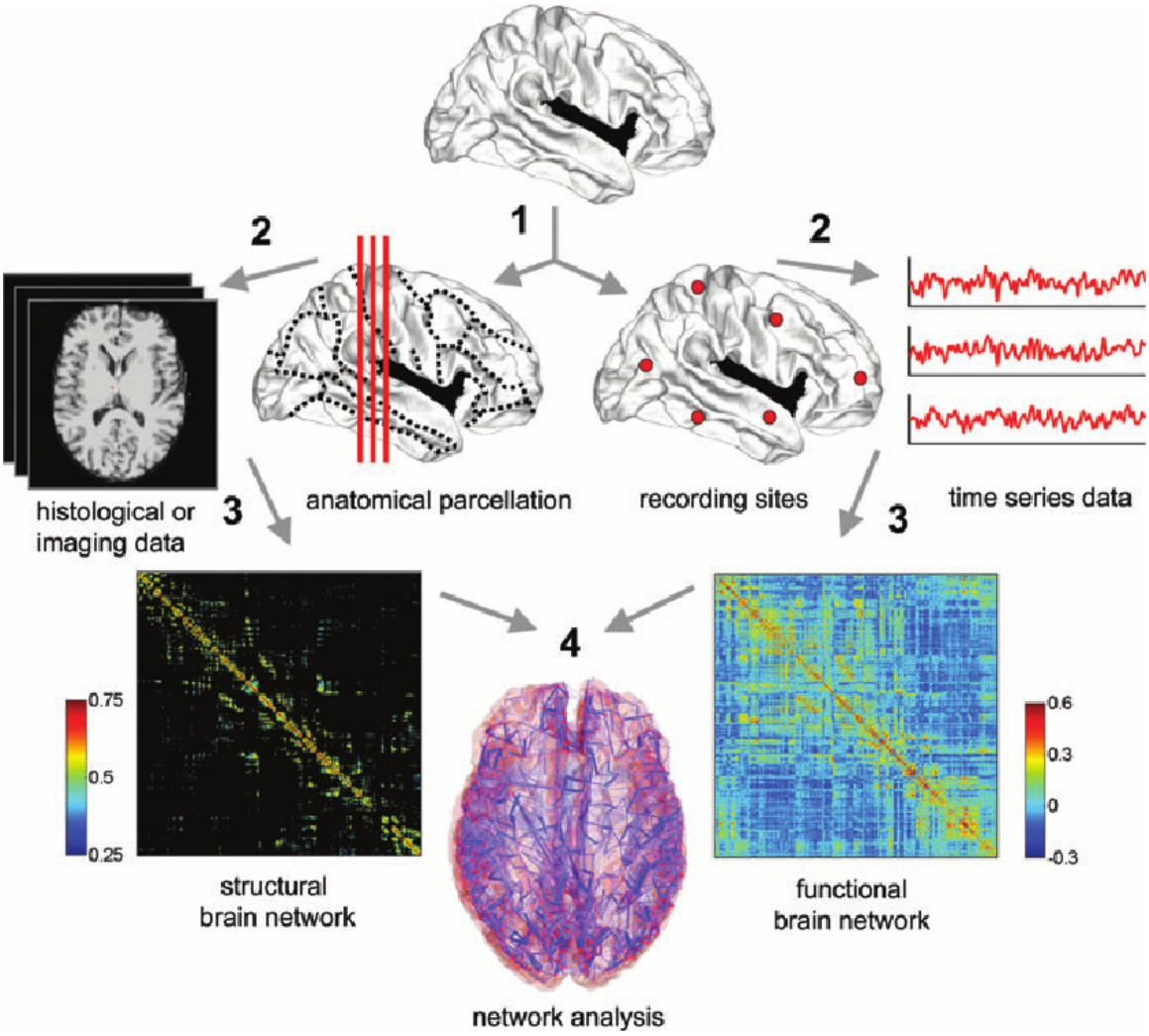

Figure 1.1: Extraction of brain networks from brain measurements and recordings. The basic workflow follows four main steps. (1) Definition of network nodes, either by parcellation of the brain volume into structurally or functionally coherent regions (left), or on the basis of placement of sensors and/or recording sites (right); (2) Definition of network edges, either by estimating structural connections from structural or diffusion imaging data (left), or by processing time series data into "functional edges that express statistical dependencies (right); (3) Network construction, by aggregating nodes and edges into a connection matrix representing a structural (left) or functional network (right) [1].

to establish statistical dependencies. Studies have provided evidence that coherence as an effective way for communication among neuronal groups [42].

To study the temporal evolution of coherence dynamics, time-Frequency global cohero-gram, a vector sum of all pairwise coherences across frequency and time, can be calculated [43, 44]. This involves segmenting time series into into small windows then computing the global coherence. Global coherences measures the extent of global coordinated activity occurring in the brain. Hence, a continuously varying coherogram.

To establish a functional link between pairwise neuronal element, a connection matrix is formed that contain all pairwise couplings as shown in figure 1.1. Coupling strengths are assigned based on the statistical dependencies between time series of distributed brain regions. Choice of association measure varies with the signal properties. Coupling can be verified by measuring the significance. A statistical significant value marks the presence or absence of a connecting link between the pairs of sources. For establishing statistical significance, these values have to survive a threshold for successfully rejecting the null hypothesis. A statistically significant connection matrix represents the presence or absence of a link between pairs of activated sources. Presence of a connecting link between binary elements is illustrated by the path of shortest distance between them. An interaction between sources can be direct or indirect i.e, connection through multiple sources. Like the anatomical connectivity, functional connectivity also constitutes a source region and a connecting link but rather than connecting directly to the other sources, there is a large amount of indirect anatomical links to the sources.

Independent component analysis (ICA) is a dimension reduction method of multivariate data, used to decompose multichannel data in into its constituent subcomponents, based on the assumption that resulting subcomponents are statistically independent. ICA method is used to assess temporal evolution of any task- evoked network [45]. Additionally, ICA is also used to nullify artifact produced by muscle activity, eye blinks and electrical noise [46].

One more method, effective connectivity, a combination of both structural and functional connectivity is used to establish directional dependencies of one neural element over another. It uses information embedded in the time series data to infer the causality direction. Examples include Granger causality [47, 48, 49], transfer entropy (detects directed exchange of information between two systems by considering the effects of the state of one

element on the state transition probabilities of the other element), dynamic causal modeling [50].

In summary, we described the methods used to explore the spatiotemporal organization of large scale functional networks underlying cognition.

Motivated by the fact that linear methods are more sensitive for coupling than non-linear methods [51] we employed linear methods for establishing a functional network as described in Chapter 2. In chapter 3 we present results of the analysis of the functional and effective network underlying 40 Hz entrainment.

Chapter 2

Methods: From EEG signals to Estimation of Brain Network Organization

"In cognitive neuroscience, the assumption is that since the brain is the source of cognitive activity, the measurement of brain electrical activity should relate to cognition in some way"
- Torello and Duffy

2.1 Introduction to EEG

The entire spectrum of humans abilities emerges by the communication between neuronal ensembles distributed within and across different cerebral regions. Neuronal elements are said to be in communication when oscillatory activity between them is phase locked to each other. Continuous interaction between brain regions can produce oscillatory activity that results in measurable electric potentials 2.1. These electrical activity can be record by placing several electrodes on the scalp according to the 10-20 system [52]. Hence, obtained electric potentials represent collective postsynaptic potentials of neuronal cells, mostly in the cerebral cortex [53]. Hans Berger in 1924 pioneered the recording of electrical activity of human brain [54]. He noticed that during wakeful relaxation with closed eyes state, mostly 8-12 Hz oscillation are contributing to EEG signals [55]. He named these oscillations alpha

rhythms. Sice then ECG has been being used as a noninvasive tool in various research domains and in clinical practice. EEG can help in diagnosing patients with epilepsy, sleep disorders, tumors and stroke by studying the unusual pattern of waves obtained. These oscillations can be classified based on the spectral content and associated cognitive behavior. Five main types are generally recognized: Alpha waves(8-13 Hz), Beta waves (15-30 Hz), Gamma waves (30-100 Hz) , Theta waves (4 - 7 Hz) , Delta waves (0.5-4 Hz). Due to very high temporal resolution (in millisecond range) EEG can be used to study evoked potentials and event related potentials.

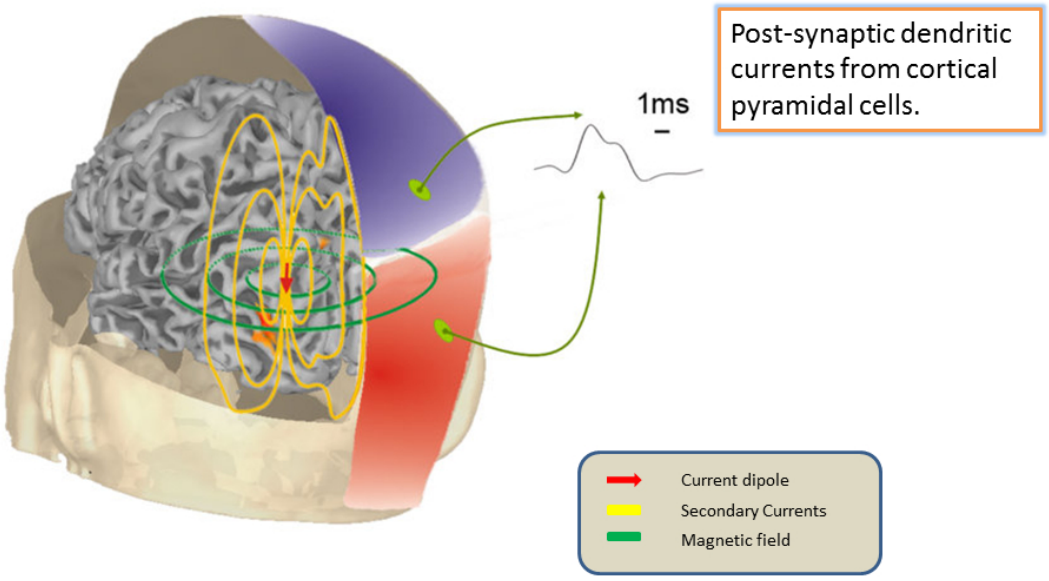

Figure 2.1: Electrophysiological principles of EEG

2.2 Event related potential(ERP)/Evoked responses(EP)

Event related potentials or ERPs are transient phasic deflections in the spontaneous activity of electrophysiological rhythm of brain, following a sensory, cognitive or motor event [56, 57]. These deflections can be monitored using a set of sensors on the scalp (e.g, by EEG or MEG). As the evoked activity can be easily obscured by large spontaneous background activities, signal averaging is carried out to delineate it. ERPs are time and phase locked

to the onset of stimuli. Characteristics of an evoked potential include amplitude (measured in mv), polarity (Negative or positive), latency period (in relation to the onset of stimuli,measured in milliseconds) and scalp distribution. Trend of ERP waveform reflect the cognitive state of brain. Hence, evoked potentials provide a non invasive measure in several clinical applications. ERPs can provide valuable insight into temporal evaluation of the information processing and dynamics of network activity in relation to a variety of different cognitive processes. N100 response during auditory stimulation is a typical example and will be elaborated in the following subsection.

2.2.1 N100 response

N100 response is a large negative evoked potential measured by EEG peaking in about 100 ms after the onset of stimulus, by any discernible auditory stimulus in absence of task demands [58]. In N100, 'N' represents negative polarity and 100 denotes the latency relative to the onset of stimuli which can vary between 90ms to 150ms. Amplitude of N100 waveform is highly dependent on the rise time of stimulus onset [59], interstimulus interval [60], stimulus intensity

[61], arousal state [62] and selective attention [63]. Though N100 ERP is primarily studied in auditory stimulation, it can also be seen in visual, somatosensory and olfactory stimulations. The generators of N100 lie in superior temporal gyri of both hemisphereswhile it is distributed mostly over the fronto-central region of the scalp [58]. N100 is associated with perceptual processing, as indicated by its frequency specificity [64].

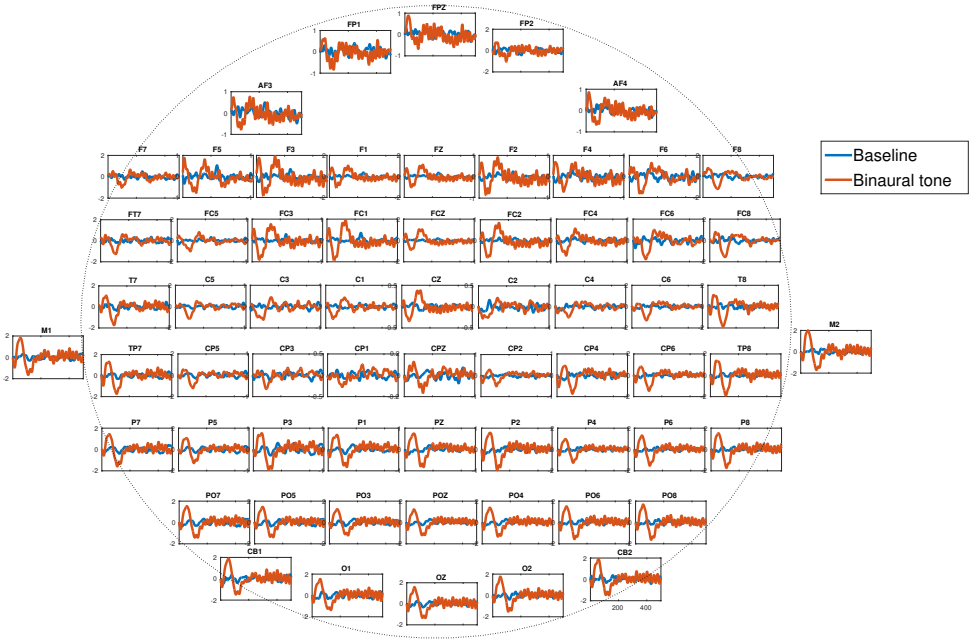

Figure 2.2: Group-averaged event related potential (ERPs) of all channels averaged over all participants and trials in rest (blue) and binaural (red) condition (refer to 3.2.2). Initial 500 ms of ERPs relative to the onset of stimuli, are plotted. A clear N100 waveform can be seen. Y axis represents magnitude (in mV), X axis represents time after the onset of stimuli.

2.3 Methods

2.3.1 Cross correlation and autocorrelation

Functional connectivity can also be estimated by measuring the temporal correlation in between two neural time series. In cross correlation analysis, correlation between two time series is measured at some displacement in time domain in relation to the first time series. Plotting correlation at each lag i.e., cross correlation, sometime referred as a *cross correlogram*. Resulting correlogram can then be interpreted as a signature of functional connectivity.

Similarly, another function *autocorrelation* is used in the analysis of EEG data wherein correlation is calculated with itself, at each lag. Whenever there is repetitive sequence in EEG time series at certain lag (which will be equal to the length of one block of repetitive

sequence), the correlation value will be high [40]. Dynamics of autocorrelation is plotted as sample autocorrelation versus time lag, referred as correlogram. A correlogram can assist in determining the auto-regressiveness of stochastic time series and measuring the proportion of randomness in time series. For a random time series autocorrelation value will be near zero.

2.3.2 Power spectrum

Power spectrum is distribution of power into frequency components composing that signal. According to Fourier analysis, any physical signal can be decomposed into a number of discrete frequencies, or a spectrum of frequencies over a continuous range [41]. Power spectrum of neurophysiological signal aids in capturing transiently stable changes in dynamics of brain response followed by a task. Generally, power spectrum of a neural signal follows pattern of $1/freq$ distribution, commonly known as pink noise. Figure 2.3 shows power spectrum during binaural presentation of periodic auditory stimuli at 40 cycles of tone (1000 Hz frequency) per sec and resting state condition.

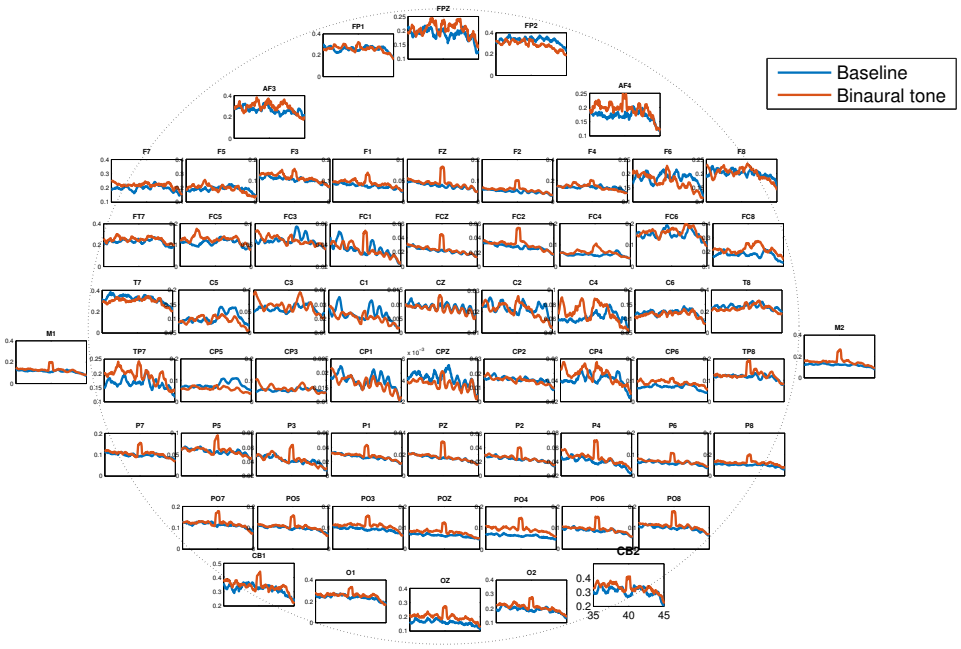

Figure 2.3: Power spectral density of all channels averaged over all participants and trials in rest in rest during binaural presentation of tone. plotted between $35 - 45Hz$. Power spectral density was calculated for 9 sec windows in each task condition.

2.3.3 Global Coherence

For inspecting the extent to which distributed neuronal assemblies are synchronizing, we employed *global coherence* analysis[43, 65]. Global coherence can be calculated from the cross spectral matrix by using the eigenvalue method. Cross spectrum as an analog of cross correlation in the frequency domain is represented by:

$$C_{ij}^{X}(f) = \frac{1}{k}\Sigma_{k=1}^{k} X_i^k(f) X_j^k(f)^* \tag{2.1}$$

where X_i^k and X_j^k are tapered Fourier transforms of the time series from the sensors i and j respectively, at the frequency f. From the obtained cross spectral matrix global was computed as the ratio of maximum eigenvalue of the cross spectral matrix to the sum of eigenvalue. i.e.,

$$C_{Global}(f) = \frac{S_1^Y(f)}{\Sigma_{i=1}^{n} S_i^Y(f)} \tag{2.2}$$

where $C_{Global}(f)$ is the global coherence, $S_1^Y(f)$ is the largest eigenvalue and the denominator $\Sigma_{i=1}^{n} S_i^Y(f)$ represents the sum of eigenvalues of the cross-spectral matrix. We used Chronux function CrossSpecMatc.m to evaluate global coherence. Global coherence was averaged over all trials. Magnitude of global coherence was used to reveal task induced multi-regional synchronization at different frequencies.

2.3.4 Phase synchrony

Synchronization between distributed neuronal ensembles subserves as a fundamental mechanism in information processing during a cognitive task [42]. Phase synchrony is employed to detect real brain interactions by using the imaginary part of coherence. Mathematically coherence is defined as a normalized cross spectrum.i.e.,

$$C_{ij}(f) = \frac{S_{ij}(f)}{(S_{ii}(f)S_{jj}(f))^{1/2}} \tag{2.3}$$

Coherence represents frequency domain analogue of correlation coefficient. Coherence value contains magnitude and imaginary part that represent amplitude and phase compo-

nents, respectively. *Imaginary coherence* circumvent artifacts that causes overestimation biases arising from volume conduction [66], a major limitation of EEG during interpreting neuronal interdependency. Imaginary coherence exploits the fact that phase similarities among time series arising from a common reference or volume conduction occur with zero time delay. Thus, by omitting the real component of coherence, which mostly contains similarities with zero time lag, we removed spurious associations and limit the analysis to the imaginary component of coherence which represents true interactions between brain areas occurring with a certain time lag.

2.3.5 Statistical tests for coherence differences

The difference between two coherence values between baseline condition and task condition at a specific frequency is calculated using Fisher's Z transformation

$$Z = \frac{(tanh^{-1}(|C_1(f)|)) - (1/d.f._{\cdot 1} - 2) - (tanh^{-1}(|C_2(f)|)) - (1/d.f._{\cdot 2} - 2)}{\sqrt{(1/d.f._{\cdot 1} - 2) + (1/d.f._{\cdot 2} - 2)}} \tag{2.4}$$

where $d.f._{\cdot 1}$ and $d.f._{\cdot 2}$ denote the degrees of freedom $(2 * N * K)$, respectively in the first and the second condition while C_1 and C_2 are coherence values at the frequency of interest. Resulting Z value was considered as an observed test statistic that was validated for significance by successful rejection of the null hypothesis. For creating a null distribution random partitions were done 1000 times by shuffling trials of two conditions and measuring coherence in each permuted data. Afterwards, a histogram is plotted comprising all 1000 coherence values from permuted data (see Figure 2.4). Observed value is then compared with the 99^{th} and 1^{st} quantile of the respective permutation distribution to validate if it is smaller than 0.1 or larger than 99.9 (threshold values were set to 1%). If observed test statistic survive threshold testing, then it reflect that the probability of getting this result by chance is 0.01. Henceforth difference is considered as significant [67].

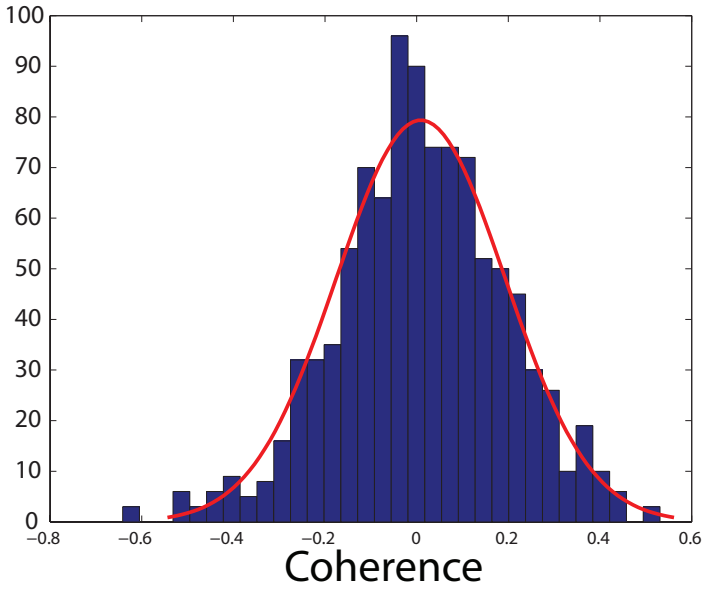

Figure 2.4: Histogram of coherence values calculated by shuffling the trials of task and rest conditions, 1000 times.

2.3.6 Granger causality

To evaluate the causal relationship in all significantly interacting channel pairs, we employed Granger's causality method. It exploit information embedded in the time series data as a fundamental tool to establish direction and strength of causal influence. Granger's causality is based on the prediction of time series of one neural time series by the temporal precedence of another time series [68].

Consider two neuronal time series X and Y be modeled as bivariate autoregressive (AR) processes of the p^{th} order

$$X(t) = \Sigma_{j=1}^{p} A_{11}(j)X(t-j) + \Sigma_{j=1}^{p} A_{12}(j)Y(t-j) + E_1 \tag{2.5}$$

$$Y(t) = \Sigma_{j=1}^{p} A_{21}(j)X(t-j) + \Sigma_{j=1}^{p} A_{22}(j)Y(t-j) + E_2 \tag{2.6}$$

where A is the coefficient matrices of model at individual lag that was calculated using multivariate Yule Walker equations, E_1 and E_2 representing two prediction errors that are independent of each other and has no temporal correlation. If after inclusion of the cross regressive equation in the univariate AR model that already have past values of current time series, the variance of the prediction error is reduced significantly then it suggests the other signal is Granger causing current signal.

Furthermore, Granger's causality can be measured in the spectral domain as explained in [69, 70]. Calculation of Fourier transformation followed by generalization of equations, spectral matrix at frequency (f), of signal X and Y is represented as

$$S(f) = X(f)Y^*(f) = H(f)\Sigma H^*(f) \tag{2.7}$$

where "*" symbolize matrix transposition and complex conjugation and $H(f) = (\Sigma_{k=0}^{m} A_m e^{-im2pif})^{-1}$ as a transfer function. Subsequently, Granger causality from X to Y represented as

$$G_{x \longrightarrow Y}(f) = -log(1 - \frac{(W_{XX} - \frac{W_{XY}^2}{W_{XX}})|H_{XY}(f)|^2}{S_{YY}(f)}) \tag{2.8}$$

where W is the covariance matrix of the prediction error, H is the transfer function, S is the cross spectral matrix of bivariate model of X and Y are neural time series, at frequency f. Similarly, one can define Granger's causality from Y to X as

$$G_{Y \longleftarrow X}(f) = -log(1 - \frac{(W_{YY} - \frac{W_{XY}^2}{W_{XX}})|H_{XY}(f)|^2}{S_{YY}(f)}) \tag{2.9}$$

After measuring causality in both directions one can locate the 'source' and 'effect' regions of brain by comparing the Granger's causality values in both the directions.

Chapter 3

Results: Large-scale Neural Network during Entrainment

"The same stream of life that runs through my veins night and day runs through the world and dances in rhythmic measures" - Rabindranath Tagore

3.1 Introduction to entrainment

When two independent physical systems oscillating at different frequencies are placed in closed proximity, they will start resonating at the same frequency after some time. This property of synchronization is known as *entrainment*. Entrainment by an external stimuli reflect a magnificent expression by nature. One such example of synchronization from our daily lives can be seen while an audience claps [71] or while we tap our feet in synchrony with the beat of a song. Furthermore, in our brain synchronous excitation of neural tissue generate oscillations as described in chapter 1 and 2. These neuronal oscillators exhibit the characterstic of entrainment by alignment of the frequency of their synchronization to the temporal dynamics of external stimuli [72]. In same context one can define *brainwave entrainment* that refers to the synchronization of the brain with the frequency of external stimuli [73]. These stimuli involved in inducing brainwave entrainment can be auditory, visual or tactile. These kind of generated neural rhythm is often phase locked to the individual cycles of periodic stimuli as presented in [74]. Therefore, entrainment seems to be a mechanism of phase alignment of the neuronal processing to temporal dynamics of

external rhythms. [75] showed the role of brainwave entrainment in inducing various mental states. Entrainment at $40Hz$ has gained maximum interest by the work of [76, 31]. They observed brainwave entrainment can be induced by presenting periodic stimuli at the rate of $40Hz$. Entrainment at $40Hz$ induces a steady state response in brain that is often exploited in measuring hearing threshold [77]. In a recent study, it has been found that entrainment to gamma rhythms (Specifically at $40Hz$) have implications to attenuate amyloid plaques in Alzheimers' mice [78]. Despite having enormous potential for theoretical and clinical applications, network underlie this phenomenon is poorly understood.

In the present study, we showed results from a novel analysis of functional networks estimated from a set of scalp EEG signals when subjects were presented with periodic auditory stimuli at $40Hz$. This study wishes to ascertain the presence of large-scale neuronal networks underlying such activities. Additionally, our aim is to see the variation in brain response during binaural stimulus and both monaural stimulus.

3.2 Experiment

3.2.1 Participants

In this experiment 21 healthy, right-handed students from National Brain Research Centre (Manesar, Haryana) ranging from 22 to 39 years of age (mean age 28 years) volunteered to participate. All subjects had normal or corrected to normal visual acuity. Informed consent were provided to all the participants. The Institutional Human Ethics Board in National Brain Research Centre approved the study protocol.

3.2.2 Stimuli and trials

Stimuli consisted of four conditions, each of 100 trials making a total duration of 200 seconds. Each trial consisted of one second of tone and one second of rest. Sounds were pure tones of 1000 Hz frequency, presented 40 times in a second as displayed in Figure 3.1 with the conditions: 1.) Binaural (in both ears), 2.) Monaural left (only in left ear), 3.) Monaural right (only in right ear) (see Figure 3.2). In addition, 4.) Baseline condition was also presented to the subjects in which there was no tone given in earphones. Subjects were instructed to stay still in sitting position and fixate at visual cross displayed on computer

screen during each condition to reduce eye movements and listen to tones attentively. When the subjects were performing experiment, electrical activity of the brain was recorded using scalp electroencephalography.

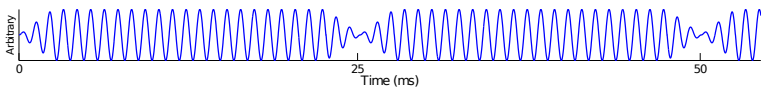

Figure 3.1: Periodic auditory stimuli having 40 cycles of 1000 Hz tone, presented in binaural, monaural right and monaural left conditions

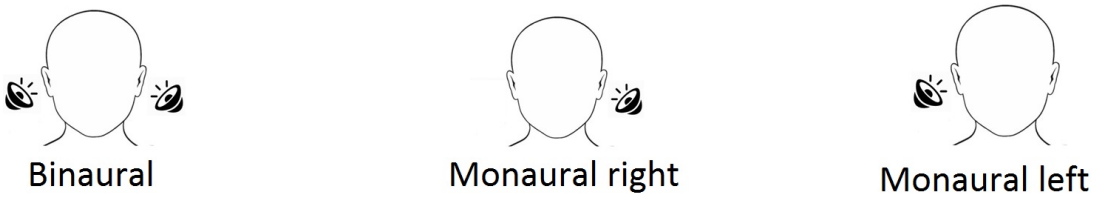

Figure 3.2: Stimuli conditions

3.2.3 Neuroimaging procedure

For recording of electrical activity, EEG with high density electrodes (64 sensors) were used. Recordings were done in a noise proof and electrically sheltered room. Recording software NeuroScan (SynAmps2) system was used, having 1 KHz sampling rate. Abrasive electrolyte gel (EASYCAP) was used to make contact with the scalp and impedance was reduced to 5k in each channel. Acoustic stimulus were given using foam inserted earphones. CZ electrode was used as a reference electrode.

3.2.4 Preprocessing of EEG signals

Epochs of 900 ms were extracted from the raw data excluding 50 ms flanking regions of time series. Obtained epochs then bandpass filtered out in the frequency range between 2 - 48 Hz. Followed by detrending (Baseline correction) of data to remove linear trends from the signal. Trials having voltage greater than $+100mv$ or lower than $-100mv$ were, considered as artifacts, therefore discarded. Furthermore, Since recordings were induces steady - state activity, we concatenated time series of ten epochs to enhance spectral resolution. This

resulted in the enhancement of contrast between noise and signal. Pre-processed data resulted in time series of 9 s with 209 trials.

3.3 Results and discussion

3.3.1 Cross correlation

Power spectral analysis revealed that right mastoid sensor (43^{th} or M2 sensor) and centro frontal sensor (10^{th} or CZ sensor) have maximum spectral power at 40 Hz. So it was assumed that this region have the most robust effect of entrainment. Hence, we performed cross correlation analysis on ERP (time series of EEG grand averaged over all trials and subjects) of M2 sensor during binaural condition. A cross correlogram is plotted in Figure 3.3. We observed a very high negative correlation at zero lag. Time series of both channels were similar, nonetheless displaying negatively correlation throughout the time series as shown in Figure 3.4. This anti-correlated may be represent the dipole formed by the voltage gradient distribution across the scalp.

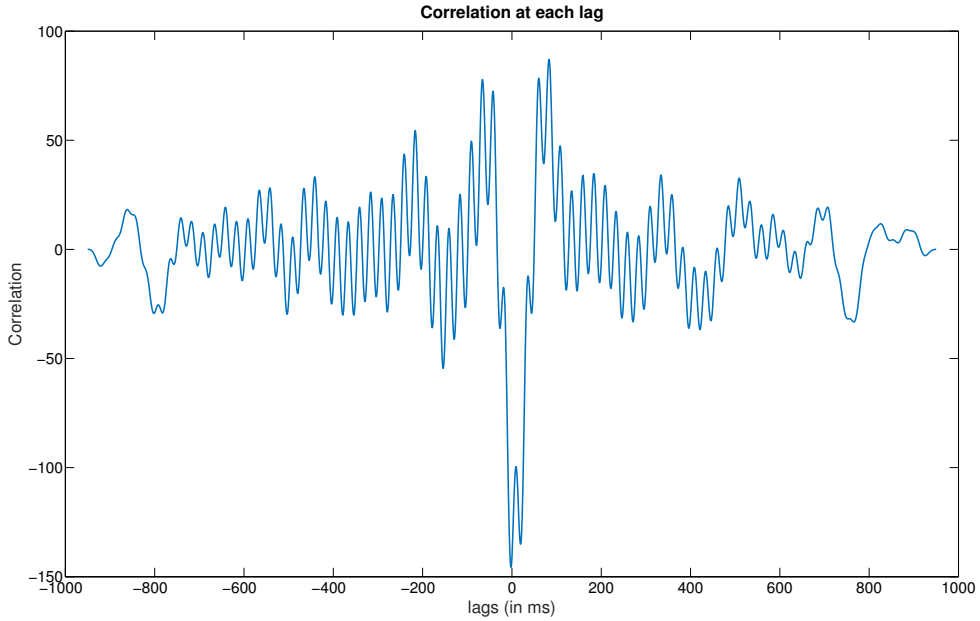

Figure 3.3: Cross Correlogram of 43^{th} and 10^{th} electrode during binaural condition.

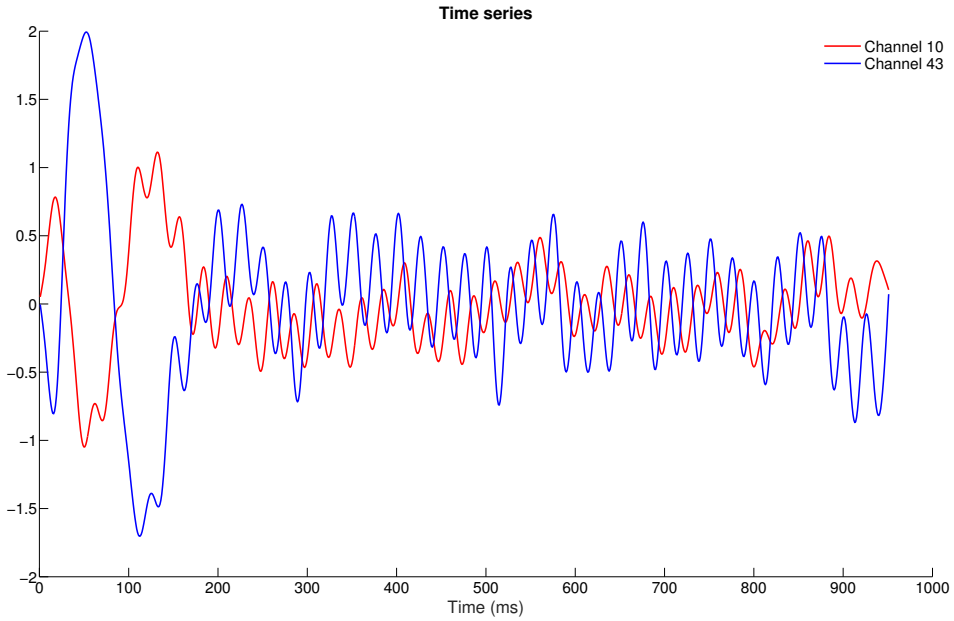

Figure 3.4: ERPs of 43^{th} and 10^{th} electrode during binaural condition. Results display a phase shift of 90° in time series with respect to other

3.3.2 Autocorrelation

We performed an autocorrelation analysis on ERP (grand averaged over all trials and subjects) of M2 sensor (showing maximum $40Hz$ spectral power) during binaural condition. A correlogram is plotted in Figure 3.5. Significance of auto correlation is determined my comparing the value with the threshold value displayed as red lines. If the autocorrelation value is higher (lower) than this upper (lower) threshold, it would be considered as significant at corresponding lag ($p < 0.05$). We found that autocorrelation values cuts off at many places, after zero lag second maximum autocorrelation obtained at lag of 63 ms relative itself. Autocorrelation analysis suggest response is coming from a non-random process. In a random data autocorrelation at every lag would be near zero.

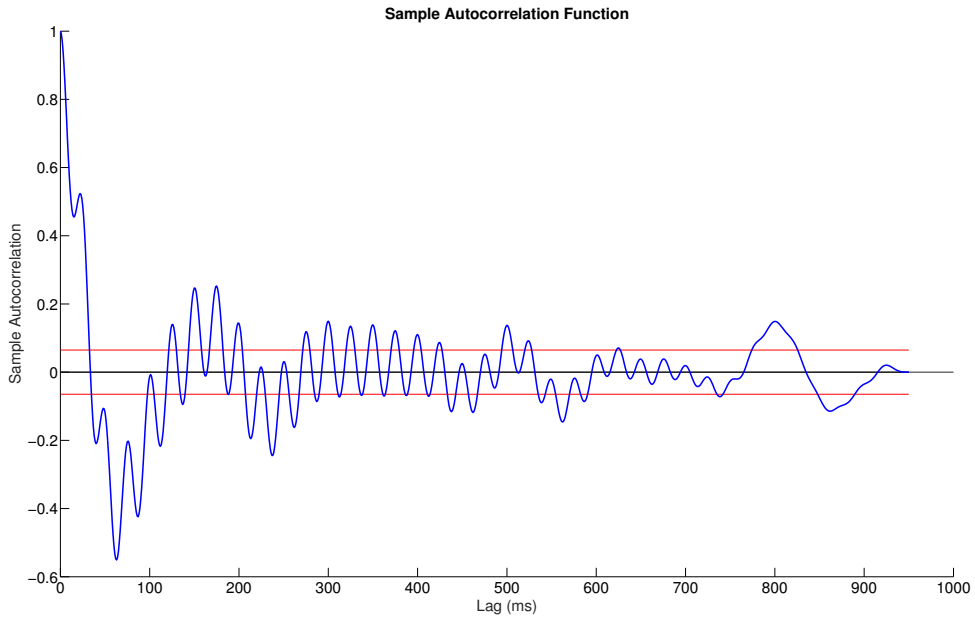

Figure 3.5: Correlogram of 43^{th} electrode during presentation of periodic auditory stimuli at a 40 tones (1Khz frequency) per sec. Red lines represent upper and lower bounds for autocorrelation with significance ($p < 0.05$).

3.3.3 Power spectrum analysis

Power spectrum were calculated for each electrode in every condition. Non-parametric statistical comparison was done to compare test conditions with baseline condition. The purple ' * ' on the topoplots marks the position of electrodes that are significantly different from the baseline condition at 99 percent confidence level. The blue areas on the scalp map highlight the regions that show decrease in the spectral power and the orange and red regions highlight the regions that show an increase in the spectral power. We observed the enhancement of spectral power at individual participant and group level at 40 Hz in distributed scalp sensor locations. Pattern of distribution of difference in the spectral power between task and rest at $40Hz$ is found to be similar in both conditions (i.e., One large cluster in frontal central areas, peripheral parieto occipital regions and in mastoid sensors). Only difference was in magnitudes in different conditions. Considering only fronto central and right hemispheric parieto occipital clusters, activity was found relatively higher in fronto central than the right hemispheric parieto occipital cluster in monaural left condition(Figure

A). This effect got reversed in monaural right condition(Figure B). In binaural condition number of significantly different sensors were higher in right peripheral parieto occipital region than compared to left peripheral parieto occipital.

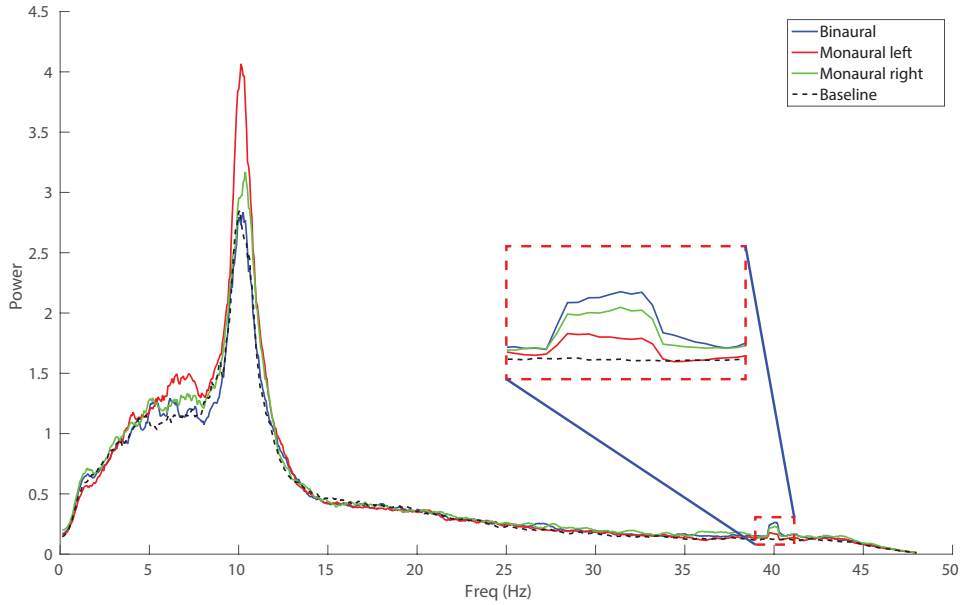

Figure 3.6: Power Spectrum averaged over all sensors, measured for monaural left (red), monaural right (green), binaural stimuli (blue) and baseline (Black dash) conditions.

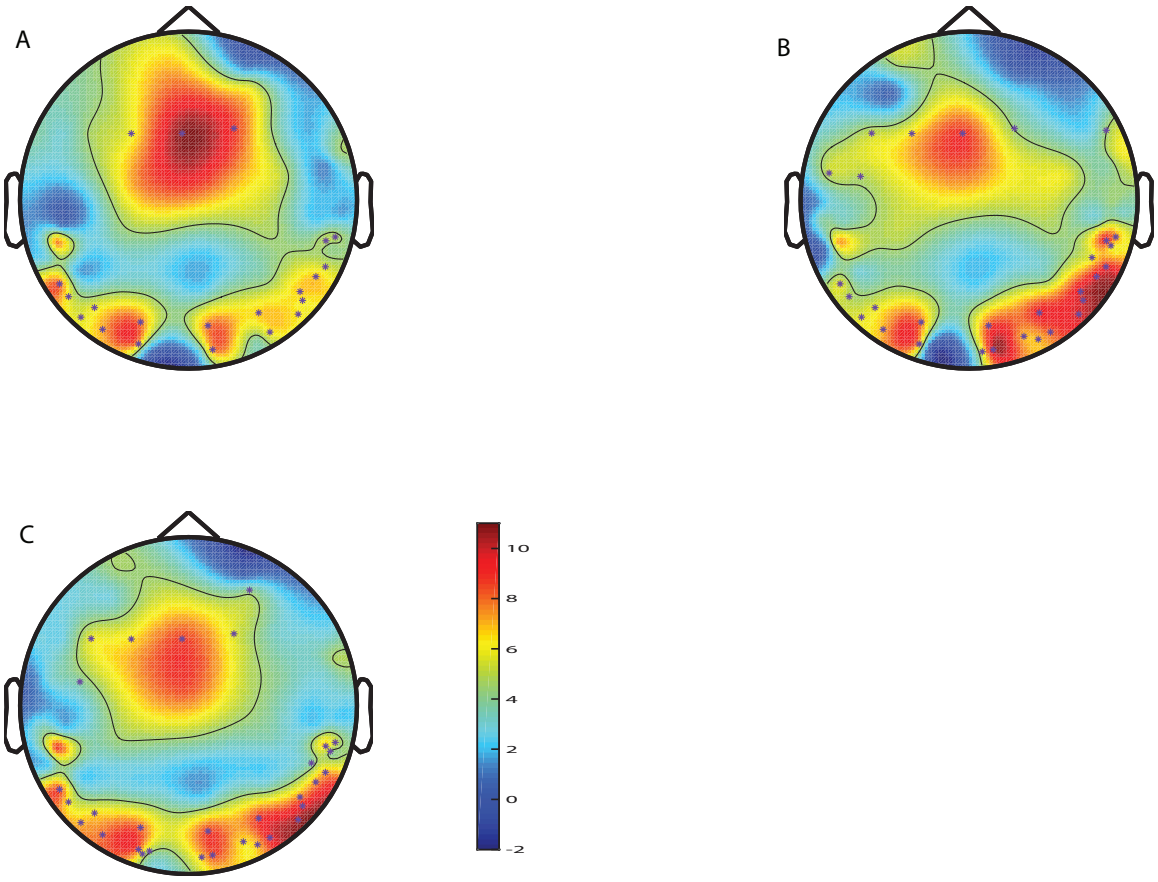

Figure 3.7: Topography and purple asterisk marks significant cluster difference ($p < 0.01$) of spectral power between task and rest at $40Hz$ during presentation of periodic auditory stimuli at a 40 tones (1Khz frequency) per sec for A) Monaural left, B) Monaural right and C) Binaural conditions.

3.3.4 Global coherence analysis

Global coherences during all conditions were calculated separately in each hemisphere across a frequency range of $2 - 48Hz$ maintaining a frequency resolution of $0.06Hz$, to reveal the influence of lateralization during different conditions. Non-parametric statistical testing were done to compare the global coherences of each hemisphere during presentation of

monaural stimuli. (Note: Central electrodes were considered as common electrodes in both hemispheres). We observed task-specific enhancement of global coherence specifically at $40Hz$ ($p << 0.01$). There was relatively higher global coherence at $40Hz$ during the presentation of monaural left stimulus in left hemisphere compared to the right hemisphere. Likewise during the presentation of monaural right stimulus global coherence was higher in right hemisphere compared to the left hemisphere (Figure 3.8 and Figure 3.9), ($p < 0.5$). Furthermore, the cumulative global coherence was more in the case of binaural tone compared to the monaural tone. To check the inter trial variability we made three partitions of the trials. One batch is from 1^{st} trial to 50^{th} trial, second from 25^{th} to 75^{th} trial and third was from 51^{th} to 100^{th} trial. The results were consistent over all trials i.e, low inter trial variability.

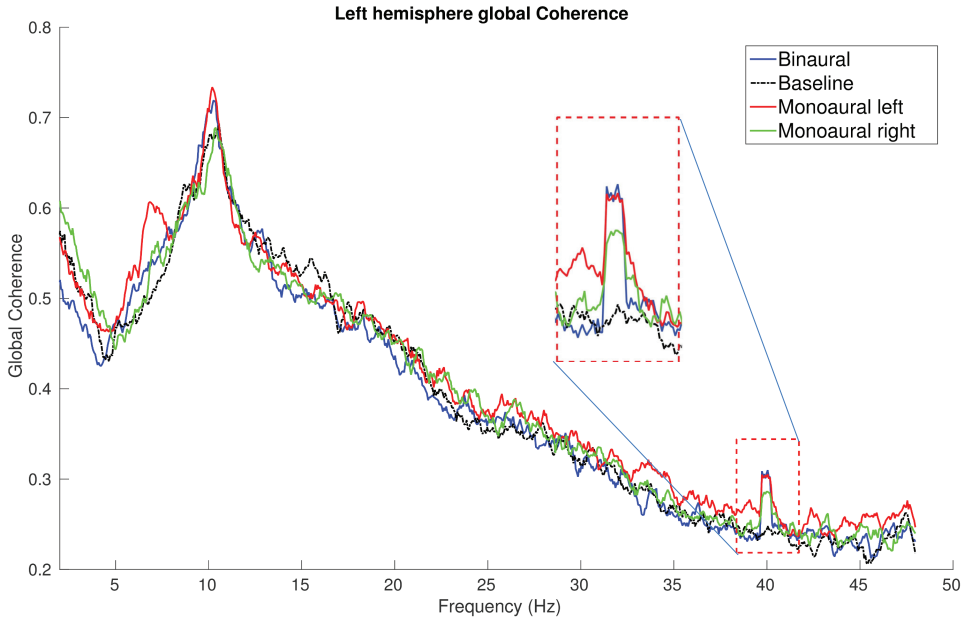

Figure 3.8: Global coherence of left hemisphere

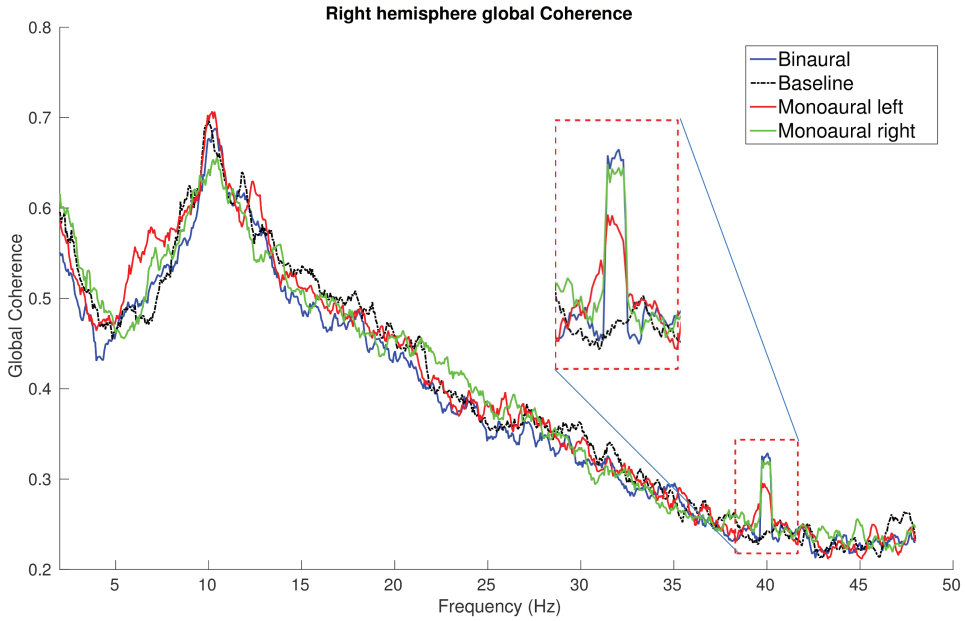

Figure 3.9: Global coherence of right hemisphere

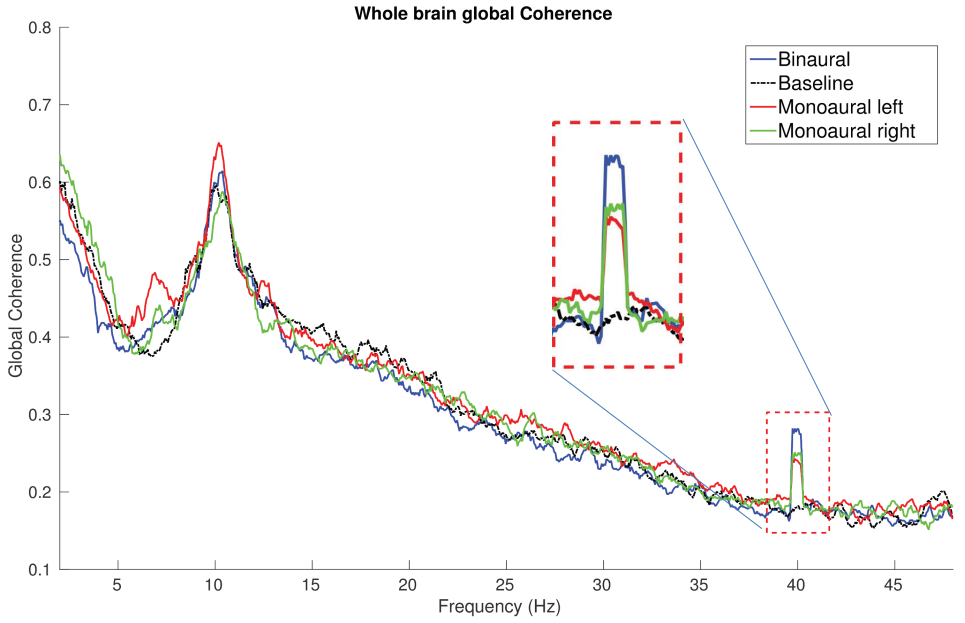

Figure 3.10: Global coherence of whole brain

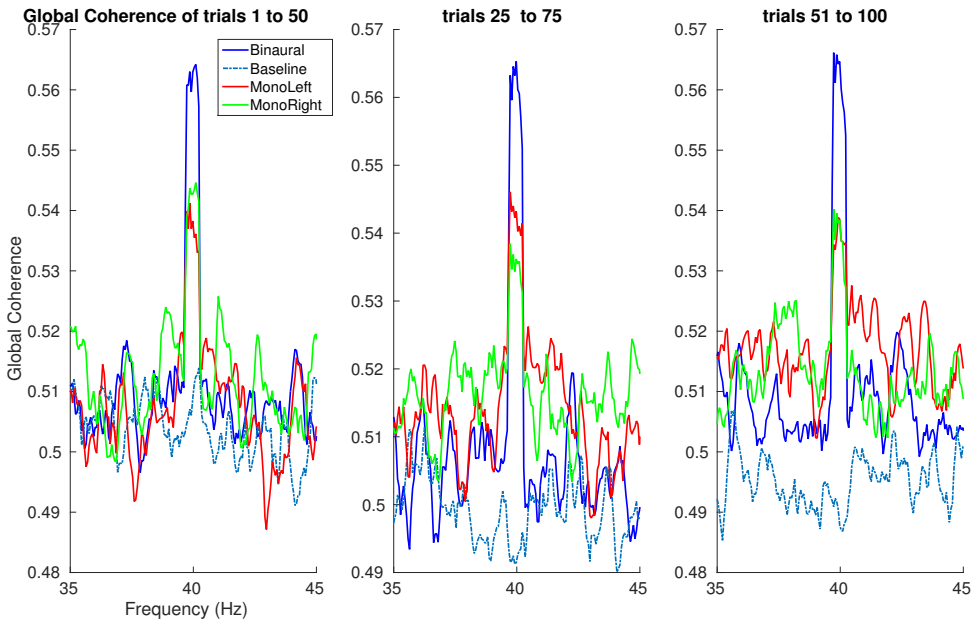

Figure 3.11: Global coherence as measured for all the conditions in three partitions by dividing trials into 1^{st} to 50^{th} trial, 25^{th} to 75^{th} trial and third from 51^{th} to 100^{th} trial.

3.3.5 Imaginary coherence analysis

Measurement of pair wise imaginary coherence was done to detect spatial dynamics of networks. A $64*64$ connection matrix containing all pairwise sensor combinations of coherence, was computed for all the conditions at $40Hz$. A coherence matrix array displays the magnitude by which two sensors coupled to each other. Imaginary part was extracted using the imag.m function of MATLAB. Connection matrix is shown in figure 3.12 Many channels have significant phase coupling with other channels at $40Hz$ ($p << 0.01$). We plotted a headmap for each condition showing all significant interaction among pairwise channels 3.13. We observed all of the interaction long range interactions between channel pairs with phase shift in oscillatory activity from frontal to occipital channel pairs. In monaural left condition there are interactions from left parieto occipital cortex to the prefrontal cortex. In monaural right condition interactions of brain areas from right hemispheric non-primary auditory cortices to the prefrontal cortex are seen. Synchrony map of binaural condition displays bilateral distribution of synchronization among channel pairs.

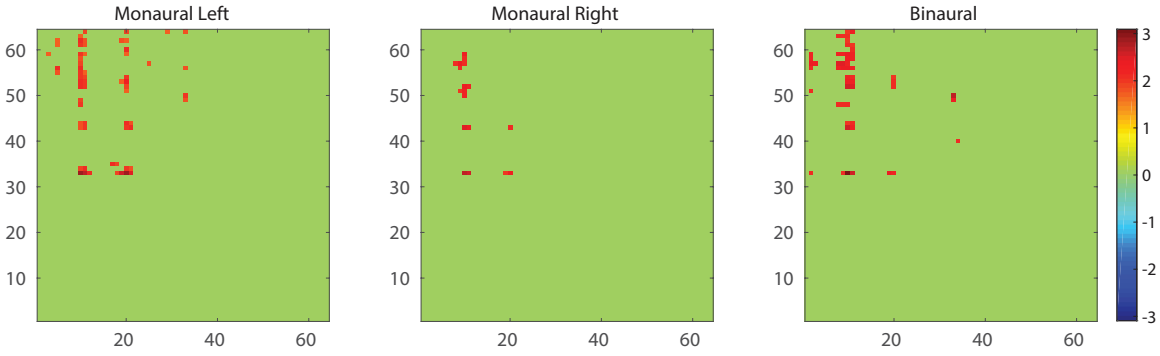

Figure 3.12: Pairwise evoked imaginary coherence in all three stimulus conditions at $40Hz$ ($p << 0.01$). Red areas representing positive phase synchrony. Non significant values are set to zero.

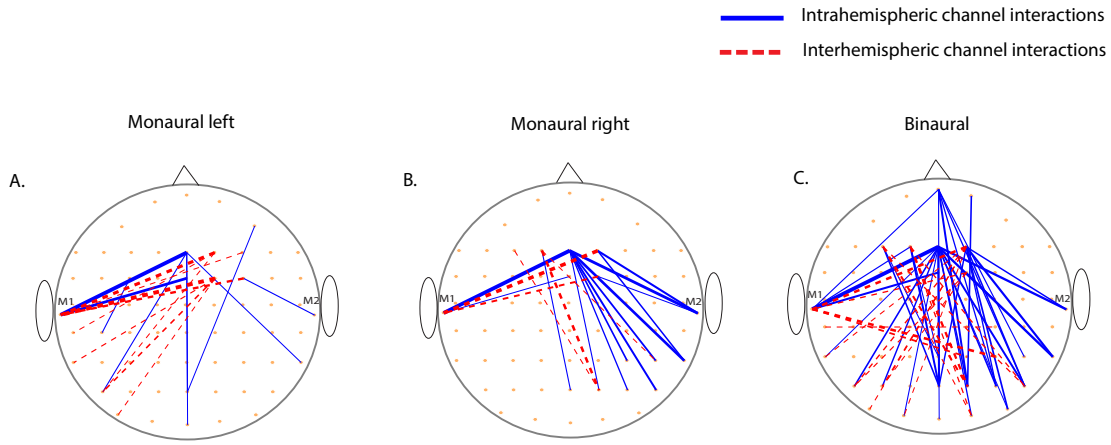

Figure 3.13: Head map depicting channel interactions during presentation of A) Monaural left B) Monaural right and C) Binaural stimuli at $40Hz$. Each blue line represents an interacting channel pair and red dashed line represents an interhemispheric channel pair interaction. The strength of interactions is represented by the thickness of the line.

3.3.6 Granger causality analysis

Since phase synchrony provides only an undirected measure of functional connectivity, to establish direction and strength of causal influence in all the interacting channel pair we

employed Granger causality (GC) method. Granger causality was measured for each conditions in all the significant interacting channel pair from imaginary coherence analysis. Statistically significant Granger causality spectral peaks were identified by a constructing random 500 permutations (as described for coherence) by shuffling trial order of electrode pair of interest. Thereafter, Granger causality was calculated for each permutation. For the electrode pair maximum GC value was identified over the frequency spectrum. Then a distribution of maximum GC values was plotted and from that distribution 99^{th} quantile value ($p < 0.01$) was set as the threshold for significance for electrode pair. Headmap was plotted for each condition illustrating the causal influence among channel pairs 3.14. A careful examination of causality network during monaural and binaural conditions revealed that a causality network during binaural condition share network dynamics with cumulative network during both monaural conditions. In binaural condition, we observed GC from the temporal region of RH is focused on the M1 region of left hemisphere (LH), through the central frontal areas, further influencing right hemisphere (RH). There are some bidirectional GC also from the frontocentral electrode to both the lateral regions of LH and RH. Since the brain attained a steady state, there may be a positive feedback loop that is subserving the brain to maintain a steady state. Bidirectional causal influence can be because of some latent driver or a common driver interacting with both electrodes. A Frontal pole to right parieto-occipital pole causality was also observed. In Monaural left condition indirect GC from the temporal region of RH to the temporal region of LH and bidirectional GC from the frontocentral sensors to parieto occipital sensors of LH was observed. In monaural right condition GC from the temporal region of RH reaches to the parieto occipital region in the same hemisphere through central frontal areas.

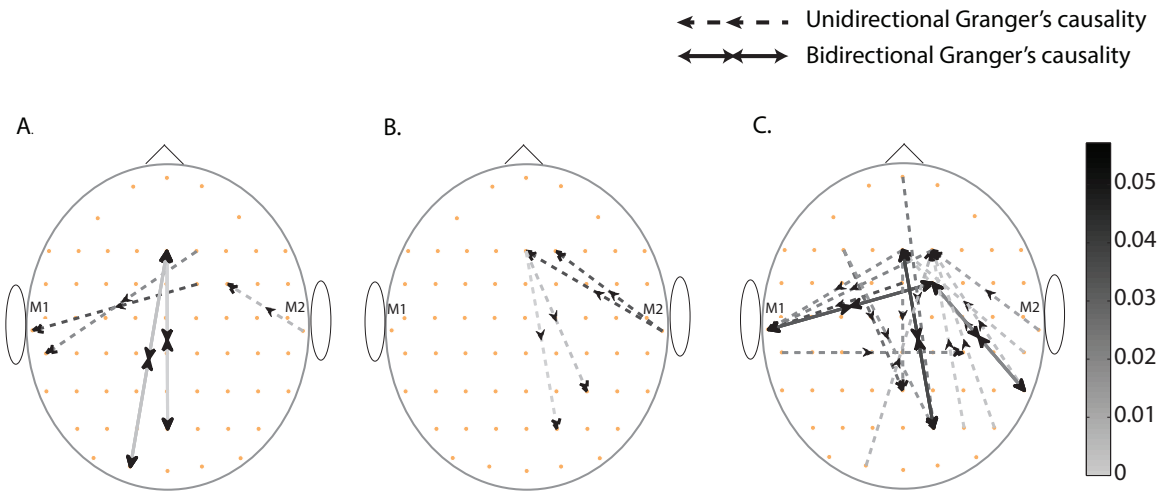

Figure 3.14: Headmap depicting causal influence between interacting channel pair (obtained from imaginary coherence analysis) during presentation of A) Monaural left B) Monaural right C) Binaural condition. Black arrows represent bidirectional causal influence between the sensors. Dashed arrows represent unidirectional causal influence in the direction of the arrow. Strength of causal influence is represented by the intensity of the color of the arrows.

Chapter 4

Conclusion and Summary

Characterizing the dynamics of the whole brain network is essential for understanding the functional organization during entrainment in brain. In the present study, we are showing results from a novel analysis of functional networks estimated from a set of scalp EEG signals when subjects were presented with periodic auditory stimuli at $40Hz$. We have shown the information processing in the brain during entrainment can be represented in terms of brain oscillations and large-scale functional brain network. We explicitly focused on investigating the characteristics of the brain network that facilitate the $40Hz$ entrainment. The main findings of the study are:

1. Entrainment of cortical areas to the frequency of presentation (i.e, at $40Hz$)

2. Recruitment of large-scale oscillatory brain networks at $40Hz$ as reflected by global coherence analysis.

3. Ipsilateral dominance in information processing networks during the presentation of monaural stimuli.

4. We found an extensive network consisting mostly long range causal interactions. This network involves causal influence from right parieto occipital sensors to the centro frontal area. Thereafter information is sent to left mastoid region, which further drive right right parieto occipital sensors.

4.1 Area specific 40 Hz steady state response

We observed the enhancement of spectral power at individual participant and group level at $40Hz$ in distributed scalp sensor locations. Clusters of enhanced spectral power was present in frontal central areas, peripheral parieto occipital regions and in mastoid sensors. Maximum spectral activity was observed in both mastoid electrodes. Transverse temporal gyrus (Heschl's gyrus) beneath the mastoid region is the first cortical structure for auditory stimulus processing. Additionally, activation in Heschl's gyrus associated with the temporal regularity of sounds [79]. This suggest that the locus of the steady state response lies in the auditory cortex. Future studies need to unravel the cortical foci of these activations using source localization methods. Power spectrum of each electrode showed a large peak at alpha band (8 to 12 Hz), in all the conditions including the the baseline condition. Alpha band oscillations has been demonstrated as the dominant frequency in the human brain and is associated with attentional processes [80, 81]. These alpha rhythms are believed to be generated by the bidirectional communication between neocortical visual areas and thalamus, reflect the electrical activity of large-scale networks [82]. Therefore, the heightened power in the alpha band can be attributed to arise from the underlying attentional network.

4.2 Presence of large scale neuro-cognitive network

Global coherence is a measure of the extent of coordinated neuronal activity over the whole brain. A large value of global coherence marks the presence of large scale brain networks (neuro-cognitive networks) underlying cognitive tasks [18]. We observed task-specific enhancement of global coherence at 40Hz, revealing an induced large-scale synchronization of neuronal assemblies at this frequency. We also observed global coherences in each hemisphere separately. There was relatively higher coherence during monaural left stimulus in left hemisphere compared to right hemisphere. Likewise, during monaural right stimulus presentation, coherence was higher in right hemisphere compared to left hemisphere. Thus, our results indicate the dominance of an ipsilateral areas underlying processing of monaural repetitive auditory stimuli. Absence of stimuli can also elicit a certain level of coherent $40Hz$ oscillation. This type of oscillations has been postulated as a mechanism of binding

of spatially distributed visual activity [83] and linked to a characteristic feature of dream state in human [31]. However, the oscillatory networks we see are of mostly primary sensory origin and most likely interact with higher order cognitive areas of frontal cortex.

4.3 Sub-networks for induced 40 Hz rhythms

We observed a task specific significant enhancement of coherent oscillations specifically at $40Hz$ compared to baseline condition. Such, long distance synchronization have been interpreted as a putative mechanism for long-range neural integration during cognitive tasks. Researchers have argued that the existence long-range synchronizations between widely separated brain regions, subserve towards "perceptual binding" [84, 85], as a framework of integration of information in distributed neuronal ensembles.

4.4 Causal interactions underlie entrainment

Granger causality was measured for each of condition and among all the significantly interacting channel pairs from imaginary coherence analysis. Statistically significant Granger causality spectral peaks were identified using non parametric statistical tests. A careful examination of causality network during monaural and binaural conditions revealed that a causality network during binaural condition share network dynamics with cumulative network during both monaural conditions. We observed that neuronal assemblies at distributed sites mostly in the sensory cortices area involving frontal central areas, peripheral parieto occipital regions and in mastoid sensors were joined in large-scale networks oscillating at $40Hz$ during maintenance of a steady state response. By distinguishing between large-scale network synchrony and that due to mutual interactions, Granger causality analysis provided a deeper understanding of cortical interaction patterns than could be obtained from synchrony measures. Grangers causality analysis reveals that both unidirectional and bidirectional causal influence is an important mechanism for brainwave entrainment at $40Hz$. In binaural condition we observed GC from the temporal region of RH is directed towards the M1 region of left hemisphere (LH), through the central frontal area which in turn influence the right temporal areas. Bidirectional GC between the frontocentral electrodes and

the lateral regions of LH and RH were also observed. This suggests that there may be a positive functional feedback loop that is subserving candidate brain regions to maintain the steady state dynamics. Bidirectional causal influence can also exist due to the presence of some latent driver or a common driver interacting with both electrodes. This can be teased out with multivariate techniques in the future. There are studies that suggest $40Hz$ entrainment is produced from the interaction of primary input in the auditory cortex and cyclic feedforward influence of nonspecific thalamic nuclei. The latter hypothesis can be supported by the presence of feedback loop and result in the activation of temporal cortex and other regions of brain [86]. Thus, the presented causality network may possibly indicate the mechanistic basis of entrainment resulting in the generation of coherent 40Hz oscillations induced by the periodic auditory stimuli.

In summary, we found stimulation by a periodic auditory stimuli at $40Hz$ entrain a large scale brain network at the frequency of stimulation and evokes a steady state response. Several theories suggest that $40Hz$ is the rhythm at which various modalities binds. The $40Hz$ oscillations may be the medium of communication over long ranges [87] thus possibly bring various percepts together and thus maintaining awareness. Exogenous entrainment of these networks are possible, as we have shown in our study. In conclusion, we establish the presence of large-scale effective network that support the entrainment, encompassing bilateral auditory and frontal areas during the processing of $40Hz$ auditory stimuli.

Bibliography

[1] O. Sporns, "The human connectome: a complex network," *Annals of the New York Academy of Sciences*, vol. 1224, no. 1, pp. 109–125, 2011.

[2] M. E. J. Newman, "Modularity and community structure in networks," *Proceedings of the National Academy of Sciences of the United States of America*, vol. 103, no. 23, pp. 8577–82, 2006.

[3] P. E. Downing, Y. Jiang, M. Shuman, and N. Kanwisher, "A Cortical Area Selective for Visual Processing of the Human Body," *Science*, vol. 293, no. 5539, pp. 2470–2473, 2001.

[4] N. Kanwisher, J. McDermott, and M. M. Chun, "The fusiform face area: a module in human extrastriate cortex specialized for face perception.," *The Journal of neuroscience : the official journal of the Society for Neuroscience*, vol. 17, no. 11, pp. 4302–11, 1997.

[5] M. N. Hart, "The Origins of Neuroscience. A History of Explorations into Brain Function," *Journal of Neuropathology & Experimental Neurology*, vol. 53, no. 5, pp. 545.2–545, 1994.

[6] S. L. Bressler and V. Menon, "Large-scale brain networks in cognition: emerging methods and principles," *Trends in Cognitive Sciences*, vol. 14, no. 6, pp. 277–290, 2010.

[7] R. Toro, P. T. Fox, and T. Paus, "Functional coactivation map of the human brain.," *Cerebral cortex (New York, N.Y. : 1991)*, vol. 18, no. 11, pp. 2553–9, 2008.

[8] A. McIntosh, "Towards a network theory of cognition," *Neural Networks*, vol. 13, no. 8, pp. 861–870, 2000.

[9] L. W. Swanson, *Brain Architecture*. Oxford University Press, 2011.

[10] A. Citri and R. C. Malenka, "Synaptic Plasticity: Multiple Forms, Functions, and Mechanisms," *Neuropsychopharmacology*, vol. 33, no. 1, pp. 18–41, 2008.

[11] W. Singer, "Development and plasticity of cortical processing architectures.," *Science (New York, N.Y.)*, vol. 270, no. 5237, pp. 758–64, 1995.

[12] S. Naik, A. Banerjee, R. S. Bapi, G. Deco, and D. Roy, "Metastability in Senescence," *Trends in Cognitive Sciences*, vol. 0, no. 0, 2017.

[13] K. Supekar, L. Q. Uddin, K. Prater, H. Amin, M. D. Greicius, and V. Menon, "Development of functional and structural connectivity within the default mode network in young children," *NeuroImage*, vol. 52, no. 1, pp. 290–301, 2010.

[14] S. L. Bressler and E. Tognoli, "Operational principles of neurocognitive networks," *International Journal of Psychophysiology*, vol. 60, no. 2, pp. 139–148, 2006.

[15] O. Sporns, "Brain connectivity," *Scholarpedia*, vol. 2, no. 10, p. 4695, 2007.

[16] K. J. Friston, "Functional and Effective Connectivity: A Review," *Brain Connectivity*, vol. 1, no. 1, pp. 13–36, 2011.

[17] R. M. Hutchison, T. Womelsdorf, E. A. Allen, P. A. Bandettini, V. D. Calhoun, M. Corbetta, S. Della Penna, J. H. Duyn, G. H. Glover, J. Gonzalez-Castillo, D. A. Handwerker, S. Keilholz, V. Kiviniemi, D. A. Leopold, F. de Pasquale, O. Sporns, M. Walter, and C. Chang, "Dynamic functional connectivity: Promise, issues, and interpretations," *NeuroImage*, vol. 80, pp. 360–378, 2013.

[18] S. L. Bressler, "Large-scale cortical networks and cognition," 1995.

[19] C. Grady, S. Sarraf, C. Saverino, and K. Campbell, "Age differences in the functional interactions among the default, frontoparietal control, and dorsal attention networks," *Neurobiology of Aging*, vol. 41, pp. 159–172, 2016.

[20] A. R. McIntosh, "Towards a network theory of cognition.," *Neural networks : the official journal of the International Neural Network Society*, vol. 13, no. 8-9, pp. 861–70, 2000.

[21] O. Sporns, D. Chialvo, M. Kaiser, and C. C. Hilgetag, "Organization, development and function of complex brain networks," *Trends in Cognitive Sciences*, vol. 8, no. 9, pp. 418–425, 2004.

[22] M. Mesulam, "Large-scale neurocognitive networks and distributed processing for attention, language, and memory," *Annals of Neurology*, vol. 28, no. 5, pp. 597–613, 1990.

[23] P. Goldman-Rakic, "Topography Of Cognition: Parallel Distributed Networks In Primate Association Cortex," *Annual Review of Neuroscience*, vol. 11, no. 1, pp. 137–156, 1988.

[24] W. J. Freeman, *Mass action in the nervous system : examination of the neurophysiological basis of adaptive behavior through the EEG.* Academic Press, 1975.

[25] J. M. Fuster, *Cortex and Mind: Unifying Cognition.* Oxford University Press, 2010.

[26] M. D. Greicius, B. Krasnow, A. L. Reiss, and V. Menon, "Functional connectivity in the resting brain: A network analysis of the default mode hypothesis," *Proceedings of the National Academy of Sciences*, vol. 100, no. 1, pp. 253–258, 2003.

[27] B. Horwitz, "Functional Neural Systems Analyzed by Use of Interregional Correlations of Glucose Metabolism," in *Visuomotor Coordination*, pp. 873–892, Boston, MA: Springer US, 1989.

[28] E. K. Miller and J. D. Cohen, "An Integrative Theory of Prefrontal Cortex Function," *Annual Review of Neuroscience*, vol. 24, no. 1, pp. 167–202, 2001.

[29] S. L. Bressler, W. Tang, C. M. Sylvester, G. L. Shulman, and M. Corbetta, "Top-Down Control of Human Visual Cortex by Frontal and Parietal Cortex in Anticipatory Visual Spatial Attention," *Journal of Neuroscience*, vol. 28, no. 40, 2008.

[30] C. M. Gray, P. König, A. K. Engel, and W. Singer, "Oscillatory responses in cat visual cortex exhibit inter-columnar synchronization which reflects global stimulus properties," *Nature*, vol. 338, no. 6213, pp. 334–337, 1989.

[31] R. Llinas and U. Ribary, "Coherent 40-Hz oscillation characterizes dream state in humans.," *Proceedings of the National Academy of Sciences*, vol. 90, no. 5, pp. 2078–2081, 1993.

[32] F. Varela, J.-P. Lachaux, E. Rodriguez, and J. Martinerie, "The brainweb: Phase synchronization and large-scale integration," *Nature Reviews Neuroscience*, vol. 2, no. 4, pp. 229–239, 2001.

[33] G. Buzsáki and J. J. Chrobak, "Temporal structure in spatially organized neuronal ensembles: a role for interneuronal networks.," *Current opinion in neurobiology*, vol. 5, no. 4, pp. 504–10, 1995.

[34] A. K. Engel, P. Fries, and W. Singer, "Dynamic predictions: Oscillations and synchrony in topdown processing," *Nature Reviews Neuroscience*, vol. 2, no. 10, pp. 704–716, 2001.

[35] B. Biswal, F. Z. Yetkin, V. M. Haughton, and J. S. Hyde, "Functional connectivity in the motor cortex of resting human brain using echo-planar MRI.," *Magnetic resonance in medicine*, vol. 34, no. 4, pp. 537–41, 1995.

[36] W. W. Seeley, V. Menon, A. F. Schatzberg, J. Keller, G. H. Glover, H. Kenna, A. L. Reiss, and M. D. Greicius, "Dissociable Intrinsic Connectivity Networks for Salience Processing and Executive Control," *Journal of Neuroscience*, vol. 27, no. 9, pp. 2349–2356, 2007.

[37] A. C. Kelly, L. Q. Uddin, B. B. Biswal, F. X. Castellanos, and M. P. Milham, "Competition between functional brain networks mediates behavioral variability," *NeuroImage*, vol. 39, no. 1, pp. 527–537, 2008.

[38] K. J. Friston, C. D. Frith, P. F. Liddle, and R. S. J. Frackowiak, "Functional Connectivity: The Principal-Component Analysis of Large (PET) Data Sets," *Journal of Cerebral Blood Flow & Metabolism*, vol. 13, no. 1, pp. 5–14, 1993.

[39] M. P. Van Den Heuvel and O. Sporns, "Network hubs in the human brain," *Trends in Cognitive Sciences*, vol. 17, pp. 683–696, 2013.

[40] M. A. Brazier and J. U. Casby, "Crosscorrelation and autocorrelation studies of electroencephalographic potentials," *Electroencephalography and Clinical Neurophysiology*, vol. 4, no. 2, pp. 201–211, 1952.

[41] J. W. Cooley and J. W. Tukey, "An Algorithm for the Machine Calculation of Complex Fourier Series," *Mathematics of Computation*, vol. 19, no. 90, p. 297, 1965.

[42] P. Fries, "A mechanism for cognitive dynamics: neuronal communication through neuronal coherence," *Trends in Cognitive Sciences*, vol. 9, no. 10, pp. 474–480, 2005.

[43] A. Cimenser, P. L. Purdon, E. T. Pierce, J. L. Walsh, A. F. Salazar-Gomez, P. G. Harrell, C. Tavares-Stoeckel, K. Habeeb, and E. N. Brown, "Tracking brain states under general anesthesia by using global coherence analysis," *Proceedings of the National Academy of Sciences*, vol. 108, no. 21, pp. 8832–8837, 2011.

[44] G. V. Kumar, T. Halder, A. K. Jaiswal, A. Mukherjee, D. Roy, and A. Banerjee, "Large Scale Functional Brain Networks Underlying Temporal Integration of Audio-Visual Speech Perception: An EEG Study," *Frontiers in Psychology*, vol. 7, p. 1558, 2016.

[45] S. Makeig, M. Westerfield, J. Townsend, T.-P. Jung, E. Courchesne, and T. J. Sejnowski, "Functionally independent components of early event-related potentials in a visual spatial attention task," *Philosophical Transactions of the Royal Society B: Biological Sciences*, vol. 354, no. 1387, pp. 1135–1144, 1999.

[46] A. Delorme, T. Sejnowski, and S. Makeig, "Enhanced detection of artifacts in EEG data using higher-order statistics and independent component analysis," *NeuroImage*, vol. 34, no. 4, pp. 1443–1449, 2007.

[47] M. Ding, Y. Chen, and S. L. Bressler, "Granger Causality: Basic Theory and Application to Neuroscience," *Handbook of Time Series Analysis*, 2006.

[48] S. L. Bressler and A. K. Seth, "Wiener-Granger Causality: A well established methodology," 2011.

[49] W. Hesse, E. Möller, M. Arnold, and B. Schack, "The use of time-variant EEG Granger causality for inspecting directed interdependencies of neural assemblies," *Journal of Neuroscience Methods*, vol. 124, no. 1, pp. 27–44, 2003.

[50] K. J. Friston, L. Harrison, and W. Penny, "Dynamic causal modelling.," *NeuroImage*, vol. 19, no. 4, pp. 1273–302, 2003.

[51] F. Wendling, K. Ansari-Asl, F. Bartolomei, and L. Senhadji, "From EEG signals to brain connectivity: A model-based evaluation of interdependence measures," *Journal of Neuroscience Methods*, vol. 183, no. 1, pp. 9–18, 2009.

[52] V. L. Towle, J. Bolaños, D. Suarez, K. Tan, R. Grzeszczuk, D. N. Levin, R. Cakmur, S. A. Frank, and J. P. Spire, "The spatial location of EEG electrodes: locating the best-fitting sphere relative to cortical anatomy.," *Electroencephalography and clinical neurophysiology*, vol. 86, no. 1, pp. 1–6, 1993.

[53] P. L. Nunez and R. Srinivasan, *Electric Fields of the Brain: The Neurophysics of EEG*. OUP USA, 2nd ed., 2006.

[54] B. Hans, "Electroencephalogram in humans," *Archiv fur Psychiatrie and Nervenkrankheiten*, vol. 278, no. 1875, pp. 87: 527– 570., 1929.

[55] E. Niedermeyer, "Alpha rhythms as physiological and abnormal phenomena.," *International journal of psychophysiology : official journal of the International Organization of Psychophysiology*, vol. 26, no. 1-3, pp. 31–49, 1997.

[56] S. J. Luck, *An Introduction to Event-Related Potentials and Their Neural Origins*. MIT Press, 2005.

[57] S. L. Bressler and M. Ding, "Event-Related Potentials," in *Wiley Encyclopedia of Biomedical Engineering*, pp. 412–415, MIT Press, 2006.

[58] R. Näätänen and T. Picton, "The N1 wave of the human electric and magnetic response to sound: a review and an analysis of the component structure.," *Psychophysiology*, vol. 24, no. 4, pp. 375–425, 1987.

[59] M. Spreng, "Influence of impulsive and fluctuating noise upon physiological excitations and short-time readaptation.," *Scandinavian audiology. Supplementum*, no. Suppl 12, pp. 299–306, 1980.

[60] H. Davis, T. Mast, N. Yoshie, and S. Zerlin, "The slow response of the human cortex to auditory stimuli: recovery process.," *Electroencephalography and clinical neurophysiology*, vol. 21, no. 2, pp. 105–13, 1966.

[61] W. D. Keidel and M. Spreng, "Neurophysiological evidence for the stevens power function in man," *The Journal of the Acoustical Society of America*, vol. 38, no. 2, pp. 191–195, 1965.

[62] A. J. Nash and C. S. Williams, "Effects of preparatory set and task demands on auditory event-related potentials," *Biological Psychology*, vol. 15, no. 1-2, pp. 15–31, 1982.

[63] S. A. Hillyard, R. F. Hink, V. L. Schwent, and T. W. Picton, "Electrical Signs of Selective Attention in the Human Brain," *Science*, vol. 182, no. 4108, 1973.

[64] R. A. Butler, "Effect of changes in stimulus frequency and intensity on habituation of the human vertex potential.," *The Journal of the Acoustical Society of America*, vol. 44, no. 4, pp. 945–50, 1968.

[65] L. C. Fonseca, G. M. A. S. Tedrus, A. L. R. A. Rezende, and H. F. Giordano, "Coherence of brain electrical activity: a quality of life indicator in Alzheimer's disease?," *Arquivos de neuro-psiquiatria*, vol. 73, no. 5, pp. 396–401, 2015.

[66] G. Nolte, O. Bai, L. Wheaton, Z. Mari, S. Vorbach, and M. Hallett, "Identifying true brain interaction from EEG data using the imaginary part of coherency," *Clinical Neurophysiology*, vol. 115, no. 10, pp. 2292–2307, 2004.

[67] E. Maris, J. M. Schoffelen, and P. Fries, "Nonparametric statistical testing of coherence differences," *Journal of Neuroscience Methods*, vol. 163, no. 1, pp. 161–175, 2007.

[68] M. Ding, Y. Chen, and S. L. Bressler, "17 Granger Causality: Basic Theory and Application to Neuroscience," *Handbook of Time Series Analysis: Recent Theoretical Developments and Applications*, pp. 380–437, 2006.

[69] J. Geweke, "Measurement of Linear Dependence and Feedback Between Multiple Time Series," *Journal of the American Statistical Association*, vol. 77, no. 378, p. 304, 1982.

[70] M. Kamiński, M. Ding, W. A. Truccolo, and S. L. Bressler, "Evaluating causal relations in neural systems: Granger causality, directed transfer function and statistical assessment of significance," *Biological Cybernetics*, vol. 85, no. 2, pp. 145–157, 2001.

[71] Z. Néda, E. Ravasz, Y. Brechet, T. Vicsek, and A.-L. Barabási, "Self-organizing processes: The sound of manyhands clapping," *Nature*, vol. 403, no. 6772, pp. 849–850, 2000.

[72] E. Niedermeyer and F. H. Lopes da Silva, *Electroencephalography : basic principles, clinical applications, and related fields*. Lippincott Williams and Wilkins, 2011.

[73] C. A. T. i. H. Huang, Tina L; Charyton and M. S. . 38-50., "A Comprehensive Review of the Psychological Effects of Brainwave Entertainment," *Alternative Therapies in Health and Medicine*, 2008.

[74] G. Moushegian and A. Rupert, "Response diversity of neurons in ventral cochlear nucleus of kangaroo rat to low-frequency tones," *Journal of Neurophysiology*, vol. 33, no. 3, p. 351, 1970.

[75] R. Fredricks, *Healing and Wholeness: Complementary and Alternative Therapies for Mental Health*. All Things Well Publications/AuthorHouse, 2008.

[76] R. Galambos, S. Makeig, and P. Talmachoff, "A 40-Hz auditory potential recorded from the human scalp.," *Proceedings of the National Academy of Sciences of the United States of America*, vol. 78, no. 4, pp. 2643–2647, 1981.

[77] O. Valentin, S. M. John, and F. Laville, "Using Auditory Steady-State Responses for Measuring Hearing Protector Attenuation.," *Noise & health*, vol. 19, no. 86, pp. 1–9, 2017.

[78] H. F. Iaccarino, A. C. Singer, A. J. Martorell, A. Rudenko, F. Gao, T. Z. Gillingham, H. Mathys, J. Seo, O. Kritskiy, F. Abdurrob, C. Adaikkan, R. G. Canter, R. Rueda, E. N. Brown, E. S. Boyden, and L.-H. Tsai, "Gamma frequency entrainment attenuates amyloid load and modifies microglia," *Nature*, vol. 540, no. 7632, pp. 230–235, 2016.

[79] R. D. Patterson, S. Uppenkamp, I. S. Johnsrude, and T. D. Griffiths, "The Processing of Temporal Pitch and Melody Information in Auditory Cortex," *Neuron*, vol. 36, no. 4, pp. 767–776, 2002.

[80] W. Klimesch, "α-band oscillations, attention, and controlled access to stored information.," *Trends in cognitive sciences*, vol. 16, no. 12, pp. 606–17, 2012.

[81] W. Klimesch, M. Doppelmayr, H. Russegger, T. Pachinger, and J. Schwaiger, "Induced alpha band power changes in the human EEG and attention.," *Neuroscience letters*, vol. 244, no. 2, pp. 73–6, 1998.

[82] R. R. Llinas, A. A. Grace, and Y. Yarom, "In vitro neurons in mammalian cortical layer 4 exhibit intrinsic oscillatory activity in the 10- to 50-Hz frequency range.," *Proceedings of the National Academy of Sciences*, vol. 88, no. 3, pp. 897–901, 1991.

[83] F. Crick and C. Koch, "Towards a neurobiological theory of consciousness," *Seminars in the Neurosciences*, vol. 2, pp. 263–275, 1990.

[84] P. R. Roelfsema, A. K. Engel, P. König, and W. Singer, "Visuomotor integration is associated with zero time-lag synchronization among cortical areas," *Nature*, vol. 385, no. 6612, pp. 157–161, 1997.

[85] G. N. Rodriguez Eugenio, "Perception's shadow: long - distance synchronization of human brain activity," *Nature*, vol. 397, p. 3, 1999.

[86] H. Weinberg, P. Brickett, A. Robertson, R. Harrop, D. O. Cheyne, D. Crisp, M. Baff, and C. Dykstra, "The magnetoencephalographic localisation of source-systems in the brain: Early and late components of event related potentials," *Alcohol*, vol. 4, no. 4, pp. 339–345, 1987.

[87] S. L. Bressler, R. Coppola, and R. Nakamura, "Episodic multiregional cortical coherence at multiple frequencies during visual task performance," *Nature*, vol. 366, no. 6451, pp. 153–156, 1993.